Available online at www.sciencedirect.com

SCIENCE DIRECT®

Cement and Concrete Research 35 (2005) 1698–1704

Cement and Concrete Research

Role of alkalis of aggregate origin in the deterioration of CAC concrete

M.T. Blanco-Varela[a,*], S. Martínez-Ramírez[a], T. Vázquez[a], S. Sánchez-Moral[b]

[a]Instituto de Ciencias de la Construcción Eduardo Torroja, (CSIC), c/ Serrano Galvache s/n, 28033 Madrid, Spain
[b]Museo Nacional de Ciencias Naturales, (CSIC), José Gutiérrez Abascal, 2; 28006 Madrid, Spain

Received 11 November 2003; accepted 26 August 2004

Abstract

Both hexagonal and cubic calcium aluminate cement (CAC) hydrates react with atmospheric CO_2, bringing about mineralogical changes in concrete, which may, on occasion, lead to loss of mechanical strength. Alkaline hydrolysis or carbonation in the presence of alkalis is a highly destructive process. The purpose of the study was to determine what caused CAC concrete deterioration in a prestressed beam that had suffered intense external damage and showed signs of alkaline hydrolysis or a reaction between the aggregate and the cement.

Samples of the internal (sound) and external (damaged) parts of the concrete were studied using XRF, XRD, FTIR, OM, SEM/EDX, and BSE techniques, and mechanical strength was measured on microspecimens extracted from both zones.

The conclusion drawn from these analyses was that alkaline hydrolysis took place on or near the surface of the concrete. The white deposits observed around the alkali-containing aggregate were found to consist primarily of bayerite whose very loose consistency undermined the aggregate–matrix bond, greatly weakening the material.

Keywords: Calcium aluminate cement; Carbonation; Alkaline hydrolysis

1. Introduction

Initially, the precipitates formed in the hydration of calcium aluminate cement (CAC) at environmental temperatures consist of the hexagonal hydrated calcium aluminates CAH_{10} and C_2AH_8. These metastable hydrates eventually recrystallize to form the cubic hydrated calcium aluminate C_3AH_6, aluminum hydroxide, and water; this is the mechanism underlying the conversion process, whose structural consequences are notorious [1,2].

Both hexagonal and cubic hydrates can react with atmospheric CO_2 [3], giving rise to hydrated carboaluminates. Likewise unstable in the presence of CO_2, the latter ultimately decomposes into a $CaCO_3$ polymorph and $Al(OH)_3$ [4,5]. CAC paste or concrete carbonation is a complex process that depends not only on the type of hydrate involved but also on the temperature, gas concentration, the amount of water available, material porosity, and so on. Carbonation may have beneficial effects on concrete strength, although the partial acid–base neutralization of the system that the process entails may trigger corrosion of the bars in reinforced concrete.

Studying the mineralogical composition of CAC samples hydrated at 4 and 40 °C and subjected to accelerated carbonation, Fernández-Carrasco et al. [5] concluded that CAC hydrate in the presence of CO_2 ultimately produces calcium carbonate in the form of vaterite and aragonite, regardless of whether the original calcium aluminate hydrates are hexagonal or cubic. Only traces of calcite were detected by the authors. Both Gaztañaga et al. [6] and Lach and Matousek [7] reported similar results in connection with the $CaCO_3$ polymorph found, and Sauman and Lach [8] identified the polymorph observed in C_3AH_6 carbonation to be vaterite. The above authors [5] also reported that the aluminum hydroxide formed when CAC pastes consisting primarily of CAH_{10} are carbonated is amorphous even 2 months after carbonation, although it subsequently recrystallizes into gibbsite, a component

---

* Corresponding author.
E-mail address: blancomt@ietcc.csic.es (M.T. Blanco-Varela).

0008-8846/$ - see front matter © 2004 Elsevier Ltd. All rights reserved.
doi:10.1016/j.cemconres.2004.08.015

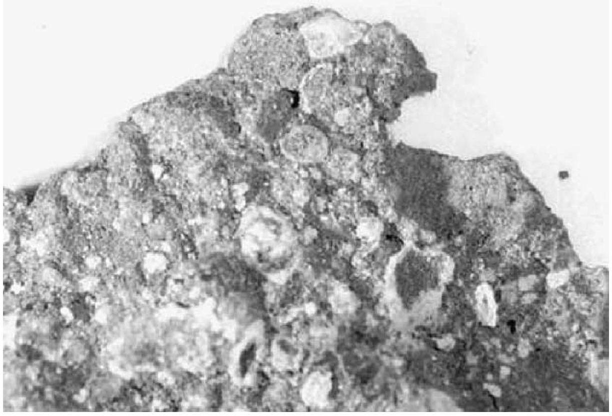

Fig. 1. Chip detached from the beam surface, with whitish spots.

associated with a substantial increase in strength. Some authors relate the presence of calcite and gibbsite as polymorphs obtained in CAC hydrate or paste carbonation to the dissolution and recrystallization of vaterite and bayerite or amorphous aluminum hydroxide, respectively. According to this theory, such polymorphs would be formed toward the end of the process and the presence of water [7,9]. Others associate the presence of calcite and bayerite with alkaline carbonation [10].

When alkalis are present in the concrete, there is a certain risk of so-called "alkaline hydrolysis", a relatively uncommon but very destructive process that affects the concrete's mechanical strength and integrity. According to Stiglitz [11], the visible signs of this phenomenon are surface cracking and scaling. The cement immediately under the surface layer is not compact and is spotted with little white dots. According to Rengade [12], this process only takes place in porous concrete and in the presence of water, as well as of alkalis and CO_2. Studying and reproducing alkaline hydrolysis in the laboratory Fernández-Carrasco et al. [13,14] found potassium dawsonite to be the intermediate product and bayerite and calcite the final products in CAC paste carbonation.

The purpose of the present study was to determine the process that led to calcium aluminate cement deterioration in a prestressed beam that was observed to have external damage of the sort described by Stiglitz [11]. This was interpreted to be a possible sign of alkaline hydrolysis that, if confirmed, would constitute the first case of alkaline hydrolysis reported in a real sample.

2. Experimental

Samples were taken from a prestressed aluminous cement concrete beam in a house located in Barcelona. The beam showed spalling, with 3 to 4 mm thick gaps where particles had crumbled away, ranging in area from 4 to 20 cm^2 (Fig. 1).

A substantial number of white spots were observed on the outer surface of this member. The outer part of the concrete mass (2–3 cm in depth) had clearly visible white spots that stood out from the darker tone of the material and that were generally found forming a ring around some of the aggregates (Fig. 2). The inside parts of the beam, on the contrary, had no such white spots and were sampled for reference as sound concrete.

The chemical composition of the internal sample was determined by XRF. The amount of water-soluble and total alkalis contained in the samples from the internal and external parts of the beams was determined by flame photometry. The samples of the two areas of the concrete were ground for FTIR and XRD determination of the mineralogical composition. Aggregates were characterized using polished thin sections examined by transmitted light microscopy. Thin sections were in part stained with Alizarin Red S to differentiate calcium carbonate phases. The samples of damaged concrete were examined with stereomicroscopy, SEM/EDX, BSE, FTIR microscopy, Raman microscopy, and polarized light microscopy.

The mechanical compression strength of the concrete in the altered and sound zones was determined using

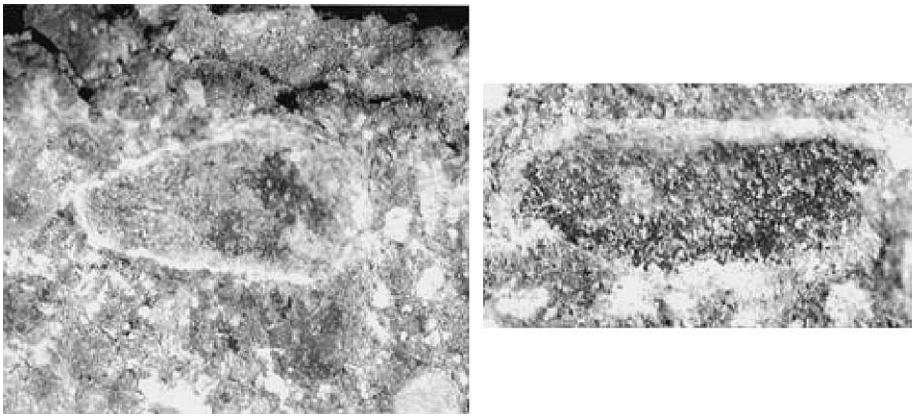

Fig. 2. Micrograph of reaction product rings around aggregates.

Table 1
Chemical analysis of concrete and ordinary CAC

	LOI	SiO_2	Al_2O_3	Fe_2O_3	CaO	MnO	MgO	Na_2O[a]	K_2O[a]	TiO_2	P_2O_5
Concrete	15.23	59.7	7.58	2.85	12.2	0.05	0.93	0.40	1.04	0.13	0.14
CAC	–	2.85	42.47	15.31	40.5	–	–	0.07	0.04	nd	nd

[a] Measured by flame photometry, nd=not determined.

cylindrical microspecimens 20 mm in diameter and 40 mm high.

3. Results

XRF analyses of a sound sample of concrete and of calcium aluminate cement are given in Table 1. The internal samples contained 0.04% of soluble Na_2O and 0.11% of soluble K_2O, whereas the external samples contained 0.09% of soluble Na_2O and 0.22% of soluble K_2O.

The mechanical compression strength of the concrete in the damaged area was 7.2±1.7 MPa, and in the sound area 16.5±0.7 MPa.

The XRD analyses of the concrete showed that the predominant phases in both the internal and external samples were quartz, calcite, micas, illites, aragonite, and a number of aluminum hydroxide polymorphs. The aluminum hydroxide in the external samples was found in the form of bayerite and nondstrandite, while in the internal samples these two polymorphs were found to coexist with gibbsite.

FTIR spectra analyses of the internal and external samples of the concrete corroborated the XRD results. The FTIR spectrum of the white reaction product ringing the aggregate is given in Fig. 3; Table 2 lists the IR absorption bands observed in the spectrum. The bands on the spectrum shown in Fig. 3 match those from calcite and the bayerite forms of $Al(OH)_3$ very closely [15].

A group of OH-stretching bands can be observed between 3000 and 3700 cm^{-1}. Such bands, which generally appear in amphoteric hydroxides, are indicative of OH groups coordinated to highly electronegative metals [14]. The various OH bands are in keeping with the crystalline structure of $Al(OH)_3$ [bayerite in this case, but also the other two polymorphs, gibbsite and nondstrandite], which consists of crystographically nonidentical (albeit very slightly different) types of Al. The bands in the high frequencies (3655 and 3620 cm^{-1}) correspond to the vibrations of free OH groups not involved in hydrogen bonding due to steric impediments. The bands characteristic of bending vibrations [δ (OH) groups appear between 1016 and 772 cm^{-1} (s, narrow)]. At lower frequencies, the intense band appearing at 532 cm^{-1} and the very weak one at 474 cm^{-1} are ascribed to out-of-plane bending vibrations. The bands at 1428, 876, and 712 cm^{-1} are calcite absorption bands and the one at 1630 cm^{-1} is a water band.

The concrete aggregates were characterized petrographically by examining thin sections under a polarized light optical microscope. The concrete consists of clasts (particles) of varying origin, immersed in a cement paste in which calcium carbonate (calcite) can be observed. Their principal characteristic, therefore, is compositional diversity and poorly selected gradation. This poor selection may be an indication that the aggregates were extracted from a torrential deposit near the sea. Most of the clasts were found

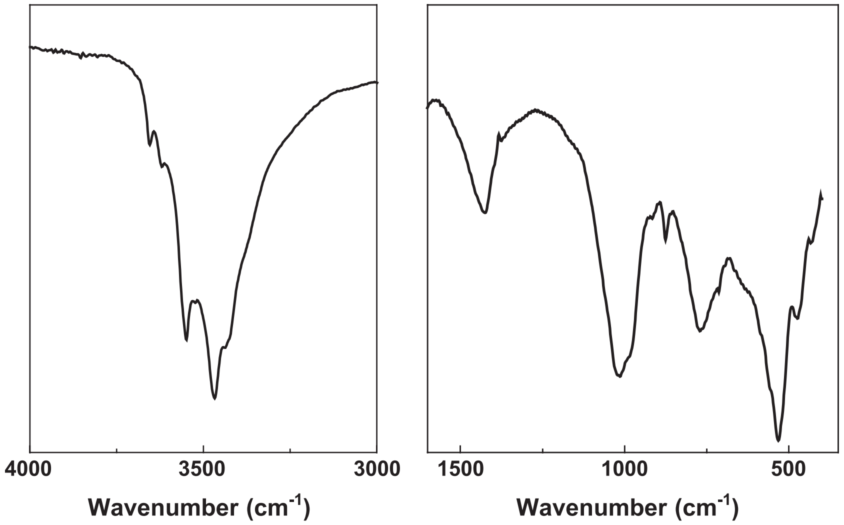

Fig. 3. FTIR spectrum of the white deposit around the aggregates on the outer layers of the concrete.

Table 2
Spectrum frequencies of the reaction product ringing the aggregates

Frequency (cm^{-1})	Intensity	Frequency (cm^{-1})	Intensity
3655	w, n.	1016	s, wi
3620	vw, n.	995	sh
3549	s, n	916	vw
3467	s, n		
3532	vw	876	w,n [$\nu_2 CO_3$]
3436	w		
3426	sh	772	m,wi
1630	w [$\nu_2 \cdot SH_2O$]	712	vw,n [ν_1 CO3]
1428	m,wi [$\nu_3 CO_3$]	532	s, n
		474	w, n

s=strong, w=weak, m=medium, vw=very weak, sh=shoulder, n=narrow, wi=wide.

to be rounded (especially the fragments of metamorphic rock), but angular grains of quartz and limestone were also found (Fig. 4).

The main components found in the sample (in descending order by proportion) were:

- Fragments of metamorphic rock: essentially schistose quartz with muscovite flakes and slate (Fig. 5).
- Grains of quartz, feldspar, and plagioclase (Fig. 6).
- Fragments of sedimentary rock: especially limestone, sandstone, and some bioclasts (fragments of brachiopod shells).
- Brownish-orange grains accumulated locally appear with parallel nicols of different morphologies whose origin did not appear to be natural due to their vitreous and isotropic texture, reminiscent of fragments of glass rich in silica, iron, and aluminum oxides.

On a whole, the sample showed relatively poor aggregate/cement bonding, as evidenced by the many gaps where particles had fallen away. Some of the metamorphic rock fragments were surrounded by rings indicative of alteration (Fig. 6).

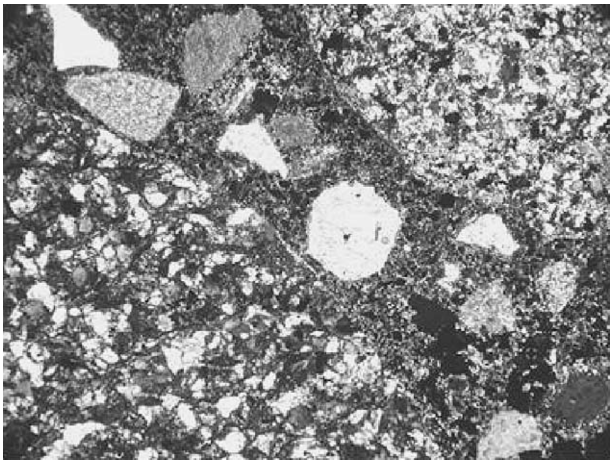

Fig. 4. View showing the compositional and textural diversity of the sample.

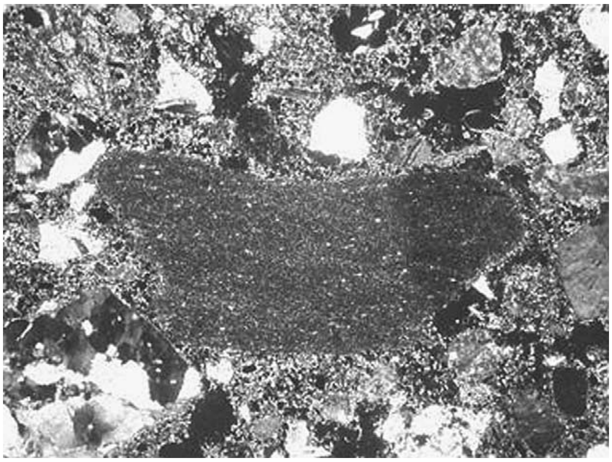

Fig. 5. In the center, a large slate fragment can be seen embedded in the paste, surrounded by other fragments of rock and quartz. Quartzite fragments, such as the one in the lower left corner, were very abundant in the sample.

The samples of deteriorated concrete were examined using SEM/EDX and BSE techniques. SEM/EDX examination of an external sample revealed the presence of particles of very diverse morphology and composition. Aggregates composed primarily of Si, Al, and K were observed, along with rounded particles essentially comprising Al (Fig. 7).

Under BSE analysis, the sample was found to contain aggregates of varying morphology and similar chemical composition (Figs. 8 and 9)— primarily Si, Al, and K— surrounded by rings that emitted a signal indicative of the presence of aluminum. Fig. 8 corresponds to an aggregate with a foliated appearance (slate) that was found on analysis to contain Si, Al, and K. Only Al was detected in the deposit around the aggregate, while paste-containing areas consisting exclusively of Ca were detected closer to the surface. Fig. 9 corresponds to an aggregate with a

Fig. 6. In the center, a sodium plagioclase embedded in the calcium carbonate cement (dyed red), surrounded by fragments of visibly altered metamorphic rock. The rings are the result of the reaction between the rock and the carbonated paste.

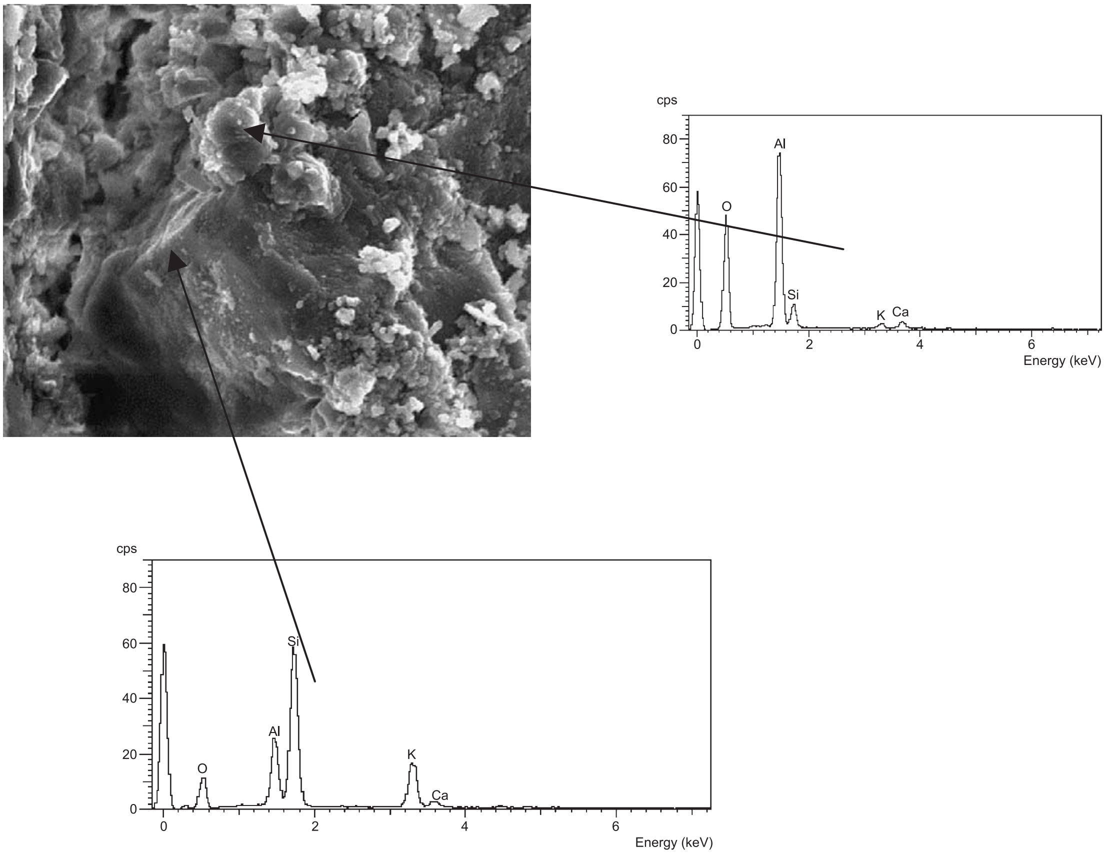

Fig. 7. SEM micrograph of an aggregate and surrounding area, and EDX analysis of the area.

smoother appearance (feldspar) than in the preceding case. Analysis showed it also comprised Si, Al, and K. Only Al was detected in the deposit around the aggregate, while paste-containing areas consisting exclusively of Ca were detected closer to the surface. The composition of the three areas described is mapped on the figure. Fig. 10 shows the space left when an aggregate was detached during sample preparation; the analysis of the visible reaction product ring showed that it contained aluminum only.

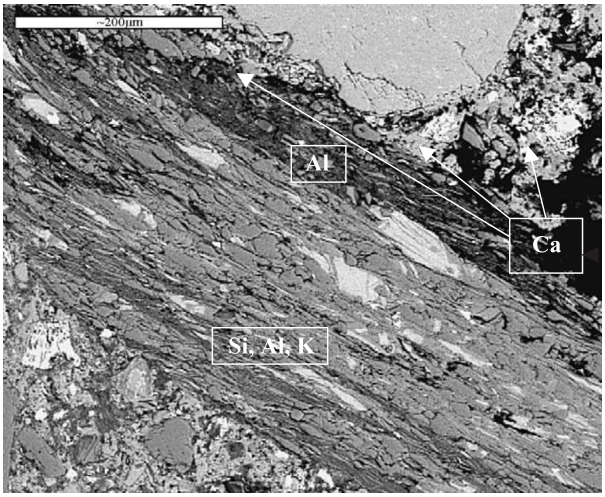

Fig. 8. Micrograph and BSE analysis of an aggregate and surrounding area.

4. Discussion

The 40-year-old beam studied was located inside a house. Chemical analysis of the concrete showed that it contained a high alkali content owing to the aggregates and that from 10% to 20% of such alkalis were water soluble. The mineralogical analyses performed on samples taken of the damaged and sound areas indicate that the cementitious matrix had no hydrated calcium aluminates, either hexagonal or cubic, and that the only phases derived from cement that we identified were aluminum hydroxide and calcium carbonate polymorphs. The concrete had, therefore, undergone carbonation with the formation of aragonite, calcite, bayerite, nordstrandite, and smaller amounts of gibbsite.

The concrete contained metamorphic-type aggregates (foliated quartz with moscovite quartz and slates), feldspar, plagioclase, and so forth, which hydrolyze in water, releasing K^+ ions in accordance with the following scheme:

$$M^+[\mathrm{Mineral}]^- + H^+ + OH^- \rightarrow H^+[\mathrm{Mineral}]^- + M^+ + OH^-$$

The binder in contact with such aggregates was exposed not only to the action of the CO_2 disseminated

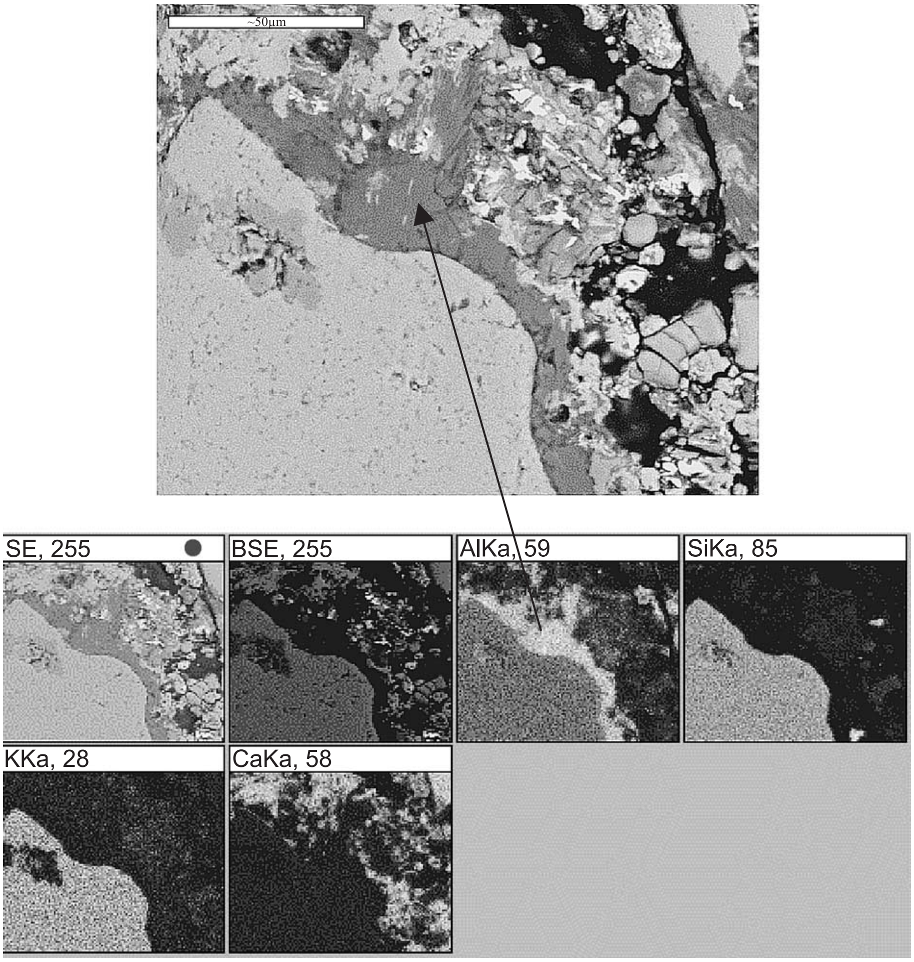

Fig. 9. Micrograph and BSE mapping of an aggregate and surrounding area.

through the pores in the concrete, but also to the K^+ released during aggregate hydrolysis, which created the conditions necessary for alkaline carbonation or alkaline hydrolysis.

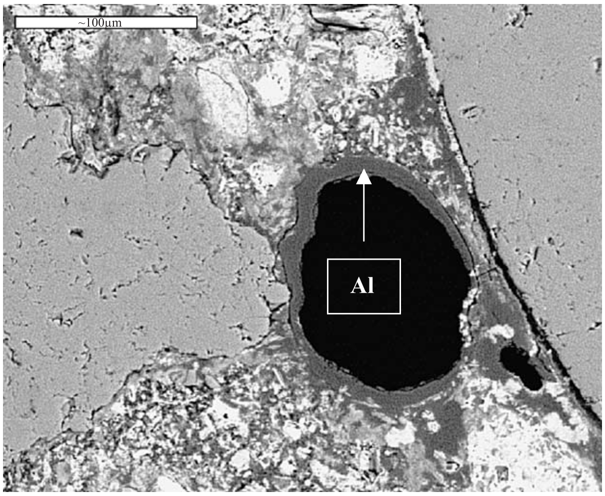

Fig. 10. Micrograph of a space left by an aggregate and the bayerite interphase.

The result was local alkaline hydrolysis on the outside of the beam, forming calcite and bayerite, primarily around the aggregates, as can be deduced from FTIR, SEM/EDX, and BSE analyses. As noted in the Introduction [12], the presence of alkalis enhances calcite and bayerite formation as the final products of CAC paste carbonation.

The scantly cohesive microstructure of calcite and bayerite, the products of alkaline hydrolysis in the samples studied, yields a very weak aggregate–matrix interphase, which would explain the loss of concrete strength. These results are consistent with laboratory findings [13,14] and correspond to the final stage of alkaline hydrolysis.

The concrete carbonated nonuniformly, with only the outermost areas near hydrolyzable aggregates affected by alkaline hydrolysis while in deeper zones where the same aggregates were present carbonation did not take place in the same manner. Since the beam was not exposed to the elements, only a limited amount of water, probably due to condensation, was available and only penetrated to a depth of about 2–3 cm via capillarity. This is the depth to which the metamorphic rock, feldspar, and so forth aggregates were found to be hydrolyzed, occasioning the subsequent alkaline hydrolysis of the CAC paste located in the immediate vicinity. Moreover, once the process was underway, the KOH produced during aggregate hydrolysis may have increased the water content via local hygroscopicity.

Further to the literature and given the scant frequency of alkaline hydrolysis, compact and low permeability concrete is generally believed not to be vulnerable to this process; nonetheless, according to Lafuma [16], high quality concrete containing soluble alkalis in aggregates such as granite would be exposed to such hydrolysis.

5. Conclusions

1. An instance of alkaline hydrolysis was identified in a prestressed CAC beam located in a residential building in Barcelona, Spain.
2. The process affected the surface layers of the material (2–3 cm) and was primarily detected around aggregates consisting of metamorphic rock, feldspar, slate, and so forth.
3. The K^+ ions released during the hydrolysis of metamorphic rock, feldspar, slate, and so forth triggered the alkaline hydrolysis observed. The water required for the reaction was presumably produced by condensation and hygroscopicity.
4. As the microstructure of the final products of alkaline hydrolysis (calcite and bayerite) deposited around the hydrolyzed aggregates was relatively noncohesive, such products constituted a weak aggregate–matrix cementitious interphase; this would explain the loss of concrete strength.

Acknowledgment

This research was subsidized under Ministry of Science and Technology grant PB1998-0518.

References

[1] C.M. Georges, Industrial aluminous cement, in: P. Barnes (Ed.), Structure and Performance of Cements, ISBN: 0-85334-233-4, 1984, pp. 415–470.

[2] P. Barnes, J. Bensted, Structure and Performance of Cements, 2nd ed., E and F N Spon, London, 2002.

[3] T. Vázquez, F. Triviño, A. Ruiz de Gauna, Estudio de la transformación del cemento aluminoso hidratado. Influencia del anhídrido carbónico, temperatura, humedad y adición de caliza en polvo, Monografía, vol. 334, del Instituto Eduardo Torroja de la Construcción, 1976.

[4] D. Damidot, S. Stronach, A. Kindness, M. Atquins, F.P. Glasser, Thermodynamic investigation of the $CaO–Al_2O_3–CaCO_3–H_2O$ closed system at 25 °C and the influence of Na_2O, Cem. Concr. Res. 24 (3) (1994) 563–572.

[5] L. Fernández-Carrasco, F. Puertas, M.T. Blanco-Varela, T. Vázquez, Carbonatación de pastas de cemento de aluminato de calcio, Mater. Constr. 51 (263–264) (2001) 127–136.

[6] M.T. Gaztañaga, S. Goñi, A. Guerrero, Accelerated carbonation of calcium aluminate paste, in: R.J. Mangabhai, F.P. Glasser (Eds.), Proc. of the Int. Conf. On Calcium Aluminate Cements, Book 0757 IOM Communications, London, 2001, pp. 349–359.

[7] V. Lanch, M. Matousek, Semin. Int. Calcium Aluminates, vol. 5, Torino, Italy, 1982, pp. 305–313.

[8] Z. Sauman, V. Lach, Long-term carbonization of the phases $3CaO.Al_2O_3.6H_2O$ and $3CaO.Al_2O_3.SiO_2.4H_2$, Cem. Concr. Res. 2 (1972) 435–446.

[9] H.G. Midgley, B.M. Woodward, RILEM Int. Symp. "Carbonation of Concrete", Wexham Springs, England, 1976.

[10] L. Fernández-Carrasco, F. Puertas, M.T. Blanco-Varela, T. Vázquez, Microstructural Development In Hydrated And Carbonated Calcium Aluminate Cement: Influence Of Alkalis And Strength Behaviour. 11th Int. Congr. Chem. Cem. (ICCC2003), In: G. Grieve, G. Owens, (Eds.), Durban (Sudafrica) 2003, pp. 1951–1959.

[11] P. Stiglitz, Utilisation du ciment alumineux dans la construction. Élimination des risques dálteration". Revue des Matériaux de Construction, n° 671–672.

[12] E. Rengade, P. L´Hopitalier, D. Fontmagne, "Reserches sur les causes de certains phénomènes dáltération des bétons de ciment alumineux". Reveu de Matériaux de Construction 378, 379, (1936).

[13] L. Fernández-Carrasco, F. Puertas, M.T. Blanco-Varela, T. Vázquez, Potassium Dawsonite formation in calcium aluminate, in: R.J. Mangabhai, F.P. Glasser (Eds.), Proc. of the Int. Conf. On Calcium Aluminate Cements 2001, Book 0757 IOM Communications, London, 2001, pp. 379–384.

[14] L. Fernández-Carrasco, F. Puertas, M.T. Blanco-Varela, T. Vázquez, Nuevos avances en la carbonatación del cemento aluminoso, "Hidrólisis alcalina", Mater. Constr. l49 (253) (1999) 47–55.

[15] Ya. I. Ryskin, The vibration of protons in minerals: hydroxyl, water and ammonium, in: V.C. Farmer (Ed.), The Infrared Spectra of Minerals, Mineralogical Society, London, 1974, pp. 144–151 Chap. 9.

[16] H. Lafuma, Quelques aspects de la physico-chimie des ciments alumineux, Rev. Gen. Sci. Appl. 1 (3) (1952) 66–74.